www.sciencemag.org/content/356/6345/eaam6892/suppl/DC1

Supplementary Materials for

Atomic structure of the human cytomegalovirus capsid with its securing tegument layer of pp150

Xuekui Yu,* Jonathan Jih,* Jiansen Jiang, Z. Hong Zhou†

*These authors contributed equally to this work.
†Corresponding author. Email: hong.zhou@ucla.edu

Published 30 June 2017, *Science* **356**, eaam6892 (2017)
DOI: 10.1126/science.aam6892

This PDF file includes:

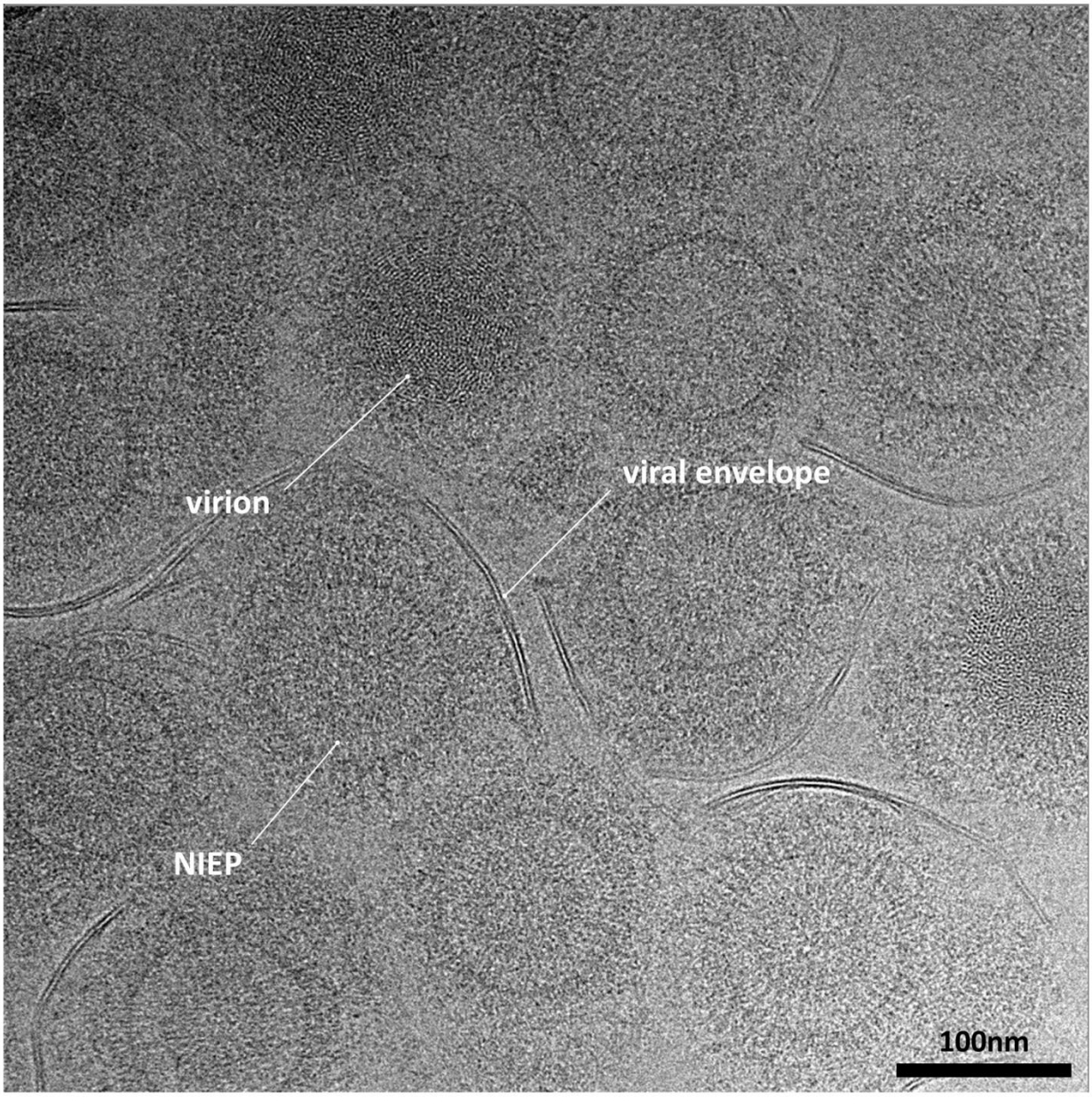

Figure S1. CryoEM imaging of HCMV particles. Image recorded using a Gatan K2 Summit direct electron detector shows two types of particles in our sample preparation: DNA-containing and DNA-devoid, corresponding to infectious virion and noninfectious enveloped particles (NIEPs), respectively. Scale bar denotes 100 nm.

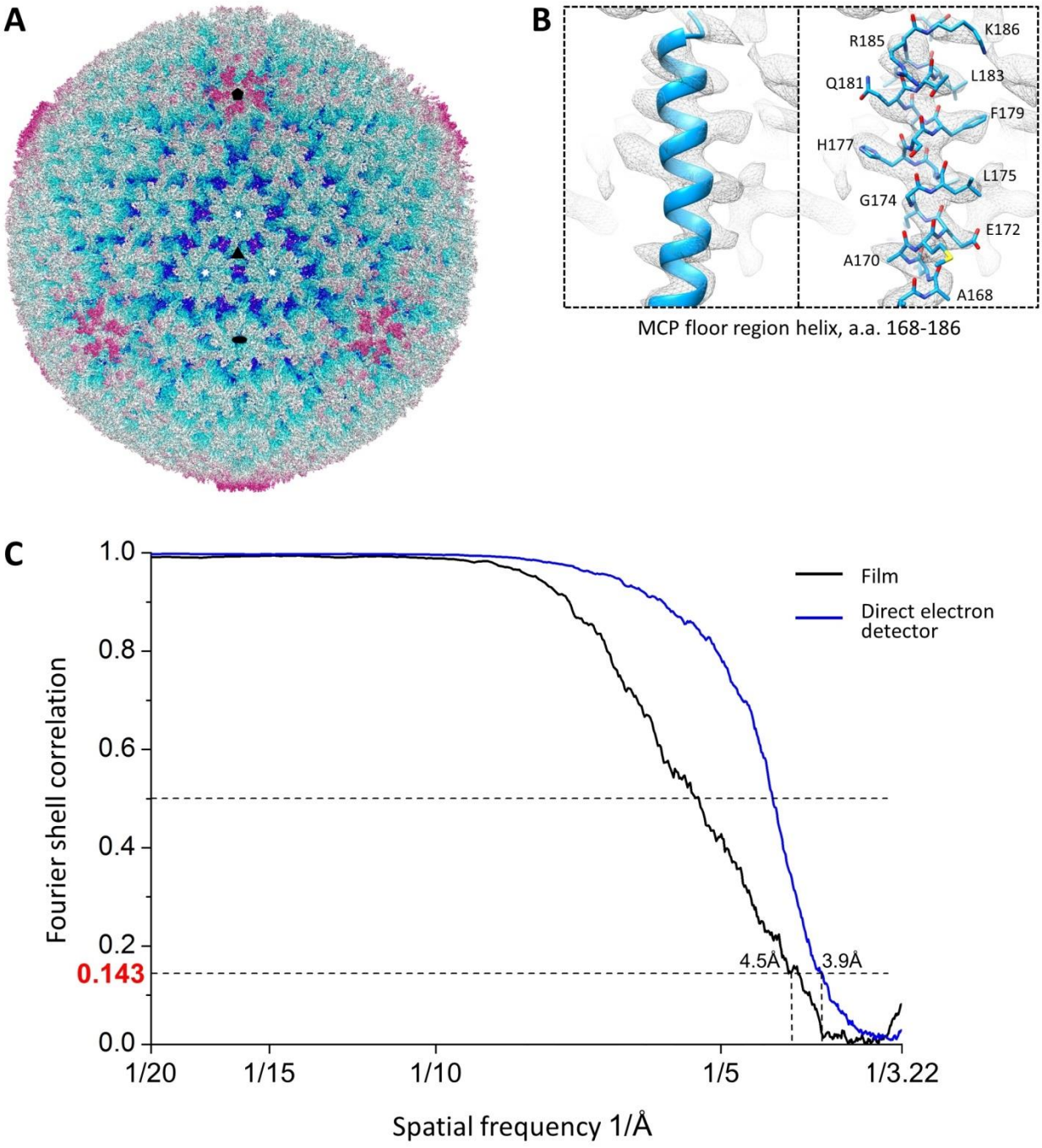

Figure S2. Reconstructions of HCMV particles and resolution assessment. (A) Radially colored 4.5-Å resolution reconstruction of HCMV obtained from film images, viewed along a threefold axis. fivefold, threefold, and twofold axes are indicated by a pentagon, triangle, and

oval, respectively. **(B)** Close-up views of MCP floor region helical density (mesh) from the 4.5-Å reconstruction superposed with ribbon and stick MCP models in left and right panels, respectively. **(C)** Comparison of resolution assessments of the initial 4.5-Å film-based reconstruction (black curve) and subsequent 3.9-Å reconstruction (blue curve) obtained from direct electron detection imaging. Resolutions were determined using a reference-based FSC coefficient criterion of 0.143.

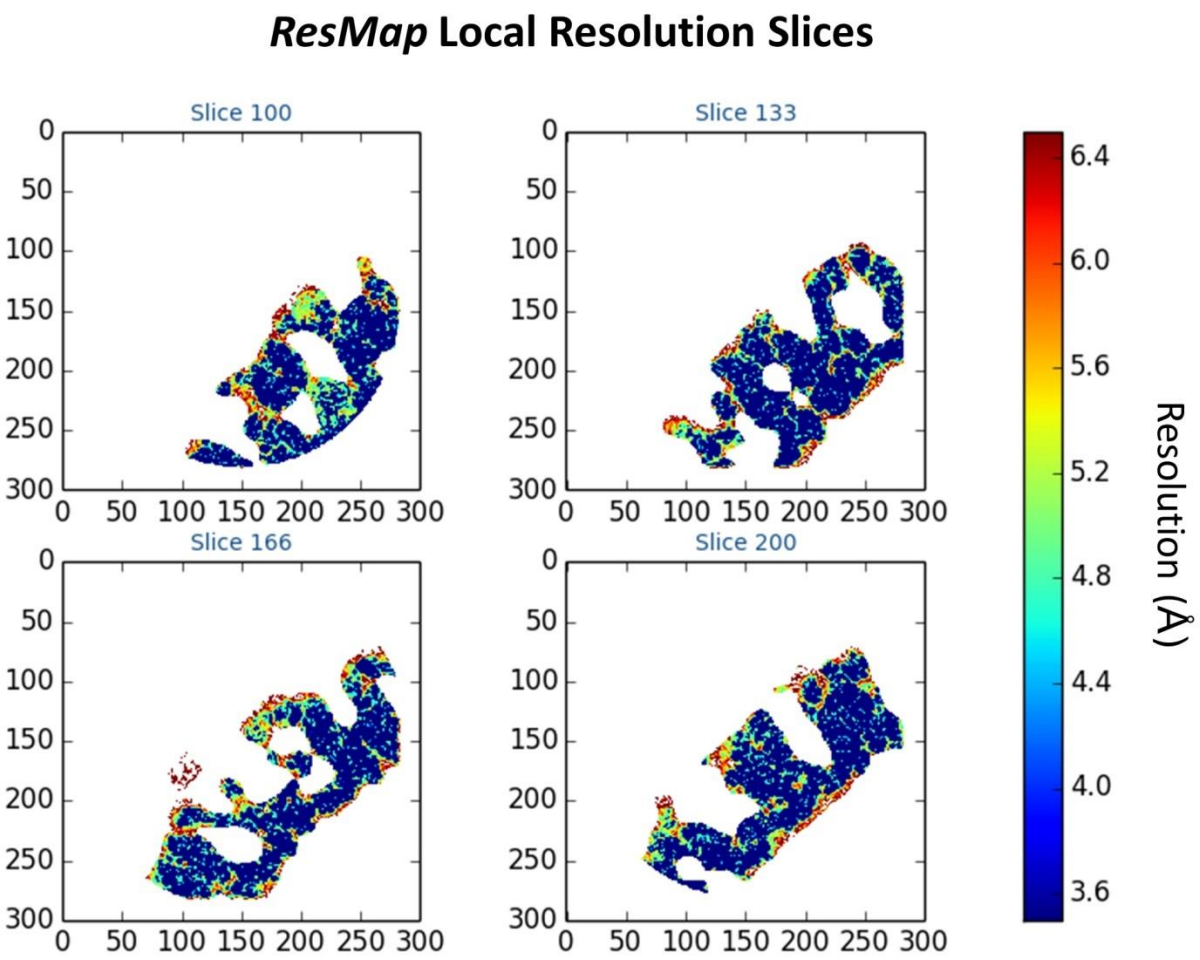

Figure S3. Local resolution assessment. Local resolution heat maps of density slices through an asymmetric unit, rendered using ResMap (*58*). The red through blue color scheme corresponds to regions of relative low through high resolution.

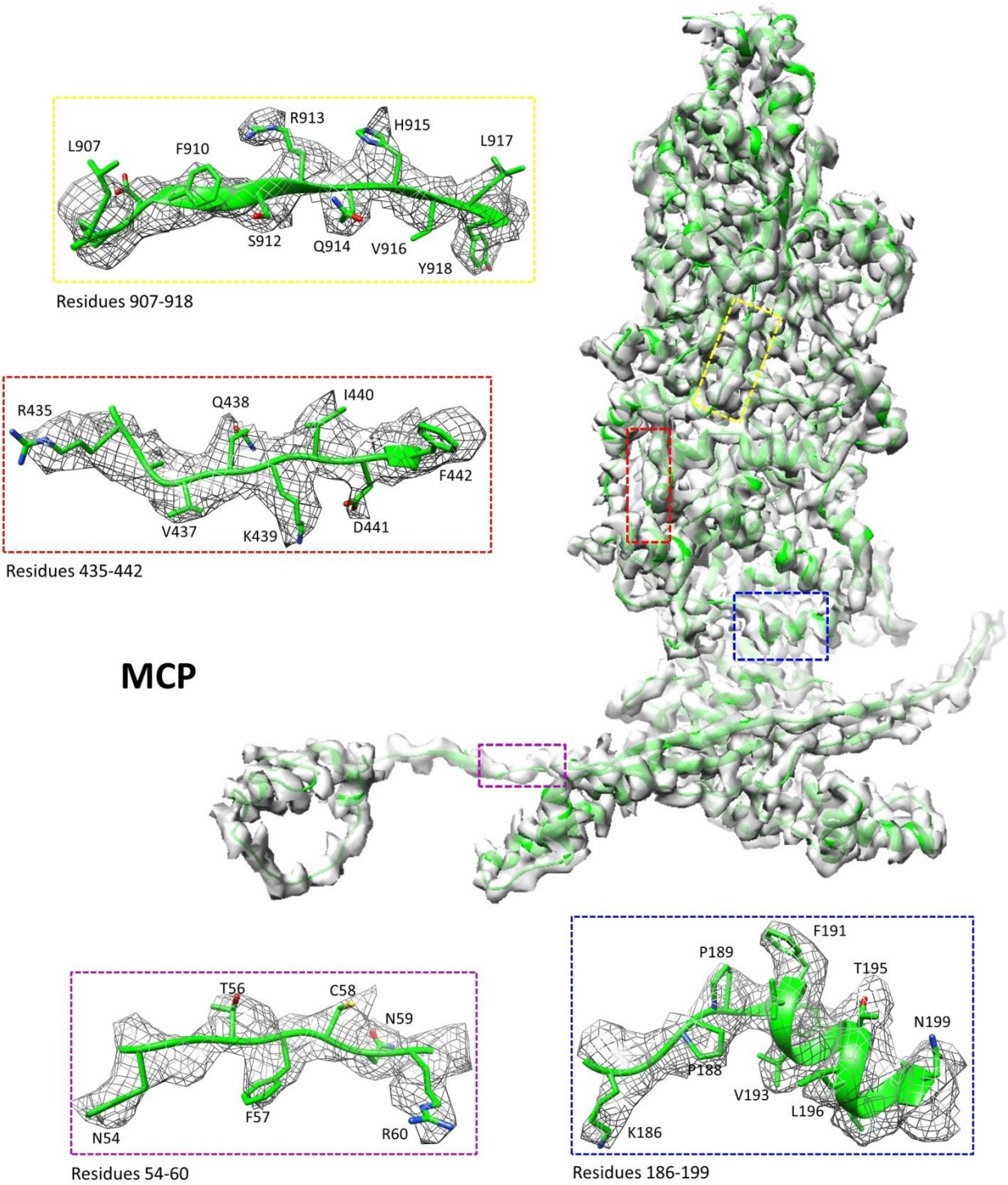

Figure S4. Density map and atomic model of MCP. Insets correspond to zoomed-in views of boxed regions and illustrate residue features in the density map (mesh).

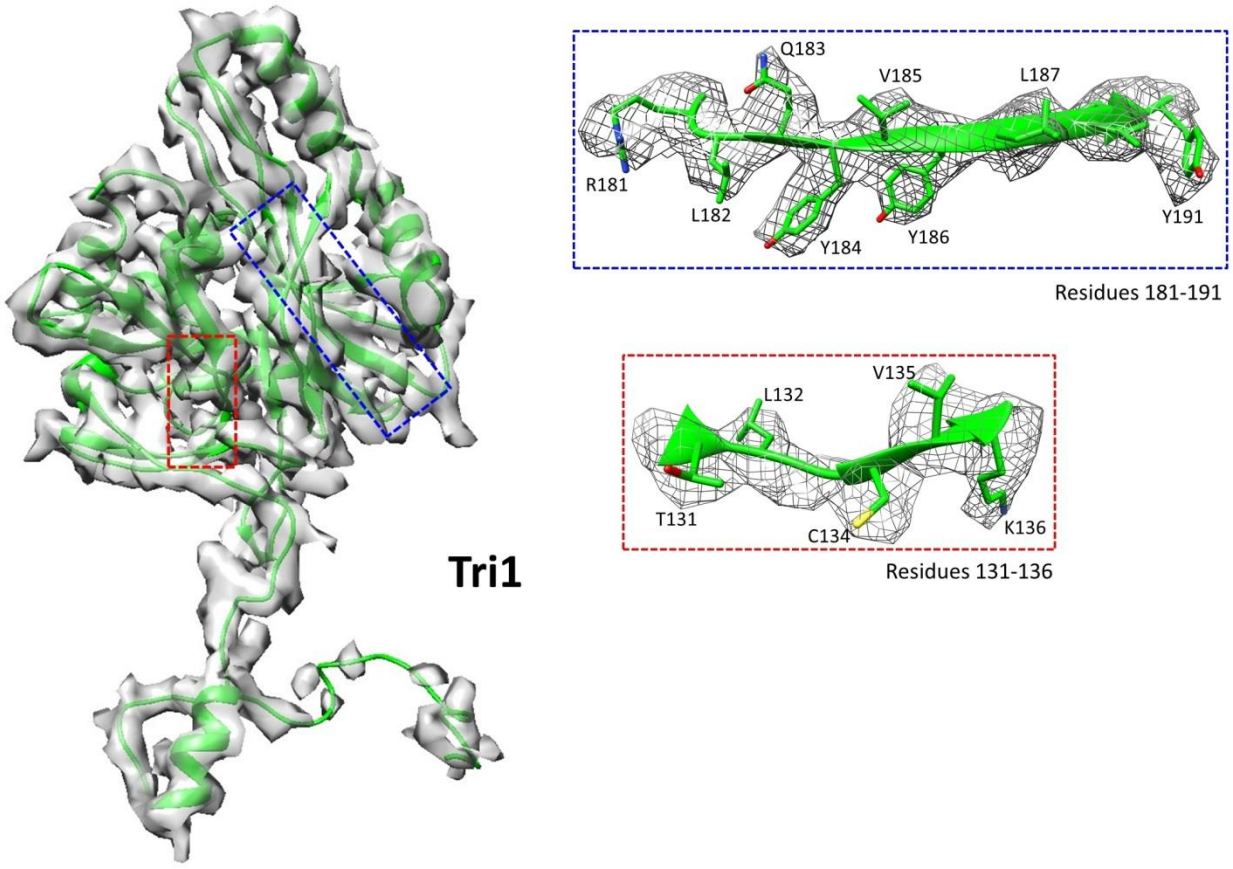

Figure S5. Density map and atomic model of Tri1. Insets correspond to zoomed-in views of boxed regions and illustrate residue features in the density map (mesh).

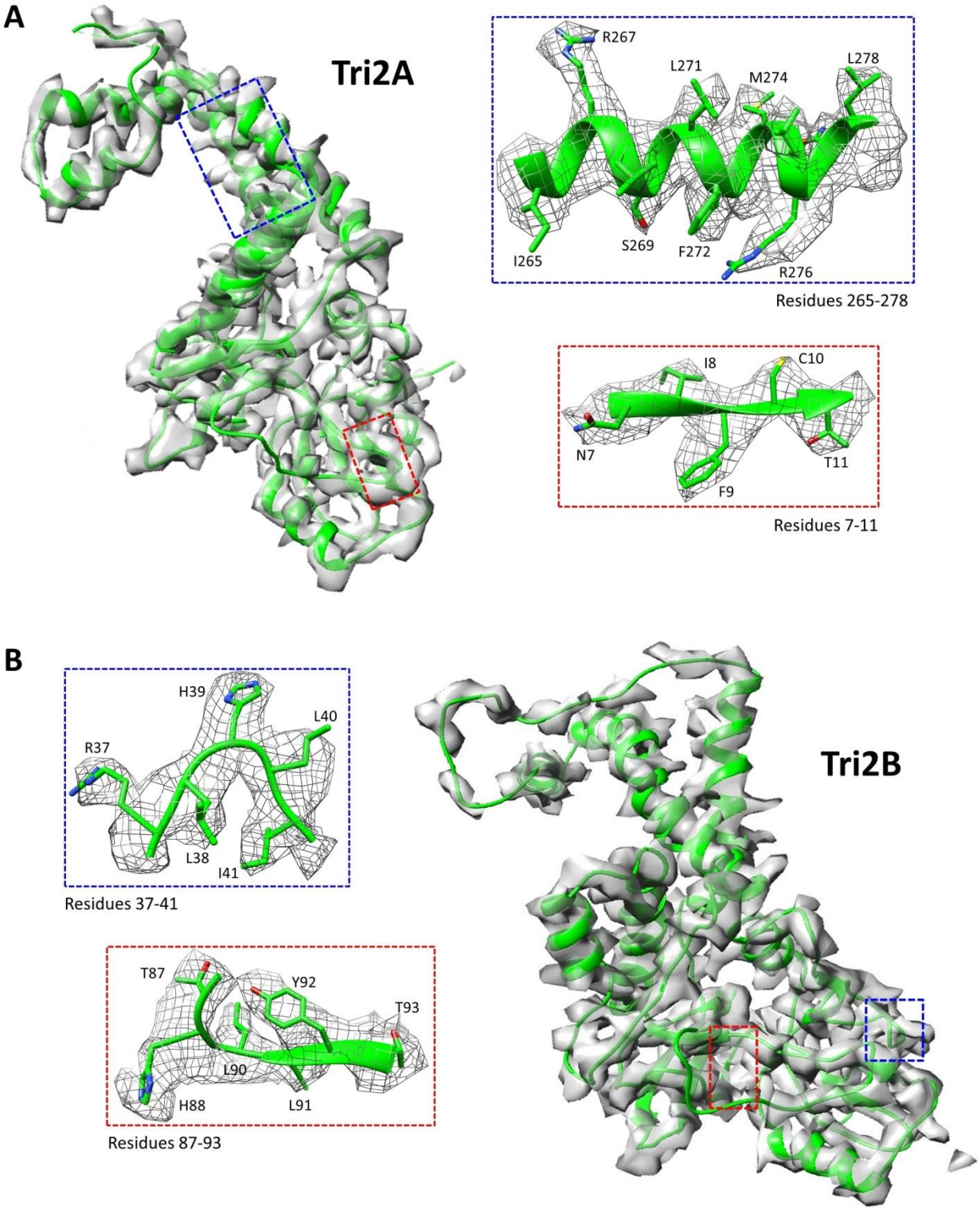
A
Tri2A
R267
L271
M274
L278
I265
S269
F272
R276
Residues 265-278
I8
C10
N7
T11
F9
Residues 7-11
B
H39
L40
R37
L38
I41
Residues 37-41
T87
Y92
T93
L90
H88
L91
Residues 87-93
Tri2B

Figure S6. Density maps and atomic models of Tri2 conformers. (A) Tri2A density map and ribbon model. **(B)** Tri2B density map and ribbon model. Insets in (A) and (B) correspond to zoomed-in views of boxed regions and illustrate residue features in the density map (mesh).

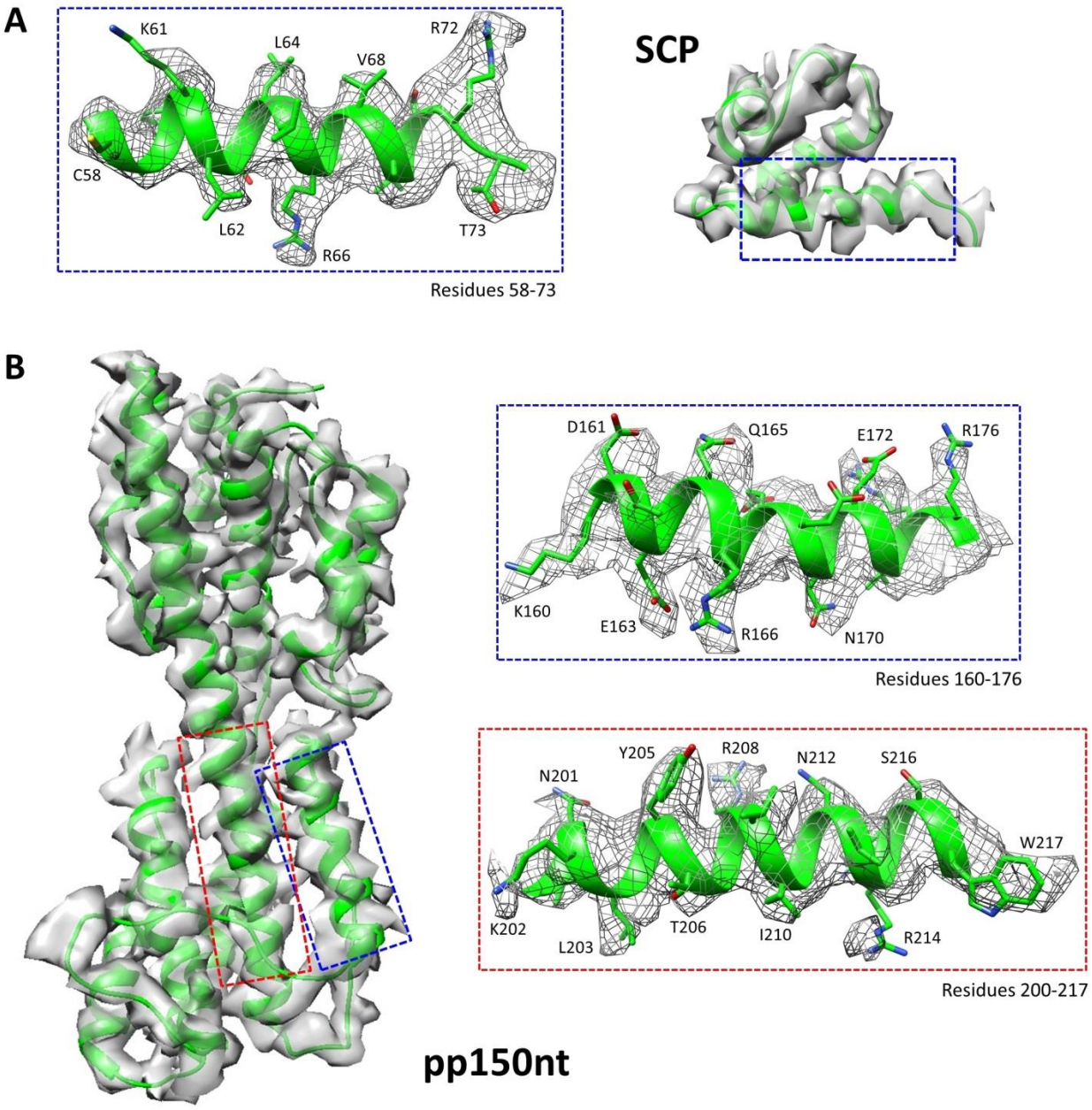

Figure S7. Density maps and atomic models of SCP and pp150nt. (A) SCP density map and ribbon model. **(B)** pp150nt density map and ribbon model. Insets in (A) and (B) correspond to zoomed-in views of boxed regions and illustrate residue features in the density map (mesh).

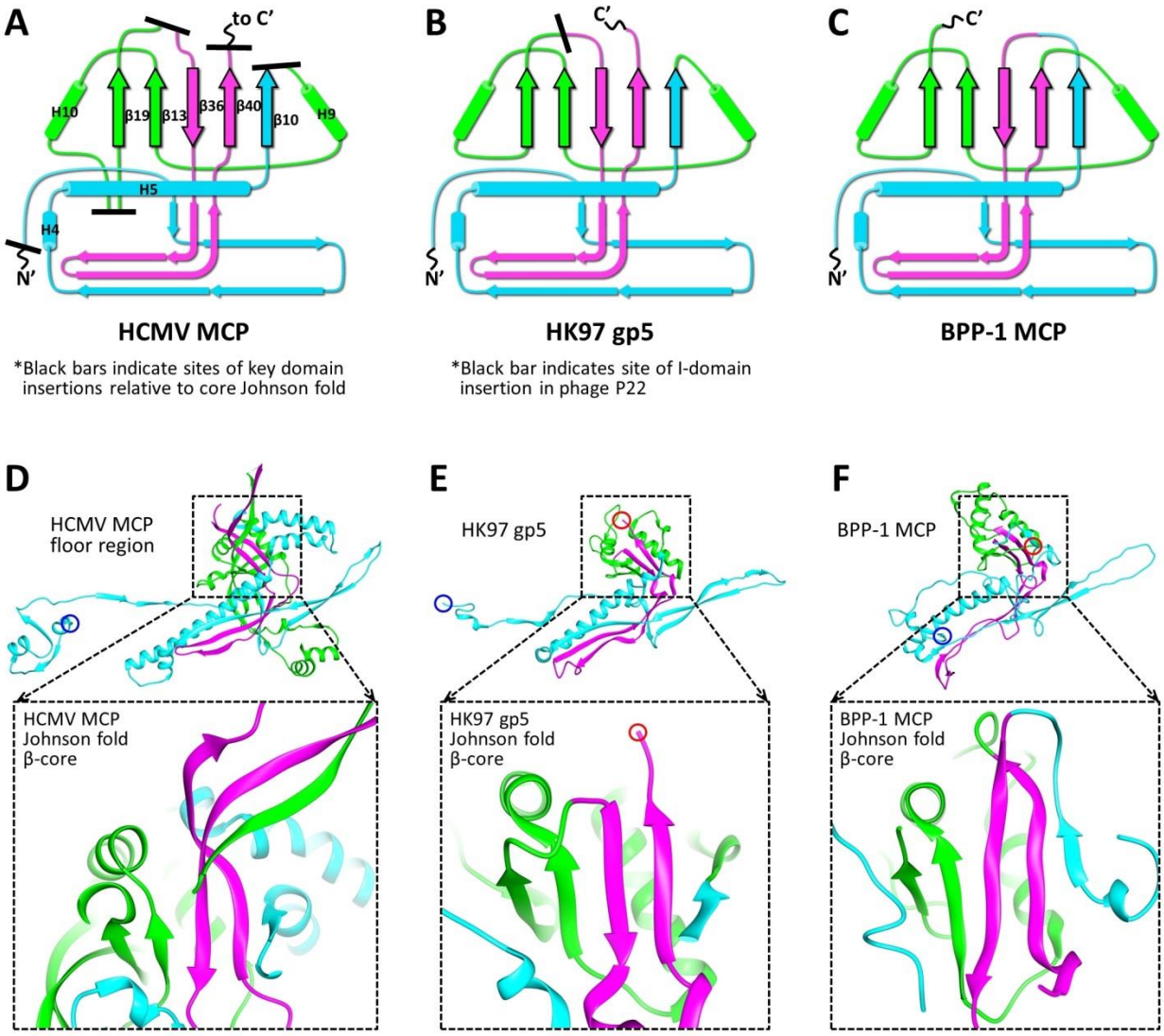

Figure S8. A comparison of Johnson fold topologies. (A-C) Schematics depict the Johnson fold organization of HCMV MCP, HK97 gp5, and BPP-1 MCP, respectively. Johnson fold N-, α-, and β-elements are colored cyan, green, and magenta, respectively. HCMV MCP and HK97 gp5 share a similar arrangement of Johnson fold elements, while BPP-1 MCP utilizes a different permutation of Johnson fold elements (*33*). Black bars in (A) indicate sites of HCMV MCP domain insertions. Black bar in (B) indicates site of I-domain insertion in phage P22 (*48*). **(D-F)**

Ribbon models of HCMV MCP, HK97 gp5, and BPP-1 MCP, respectively, colored by Johnson fold element as in (A-C). Insets depict their respective Johnson fold β-cores.

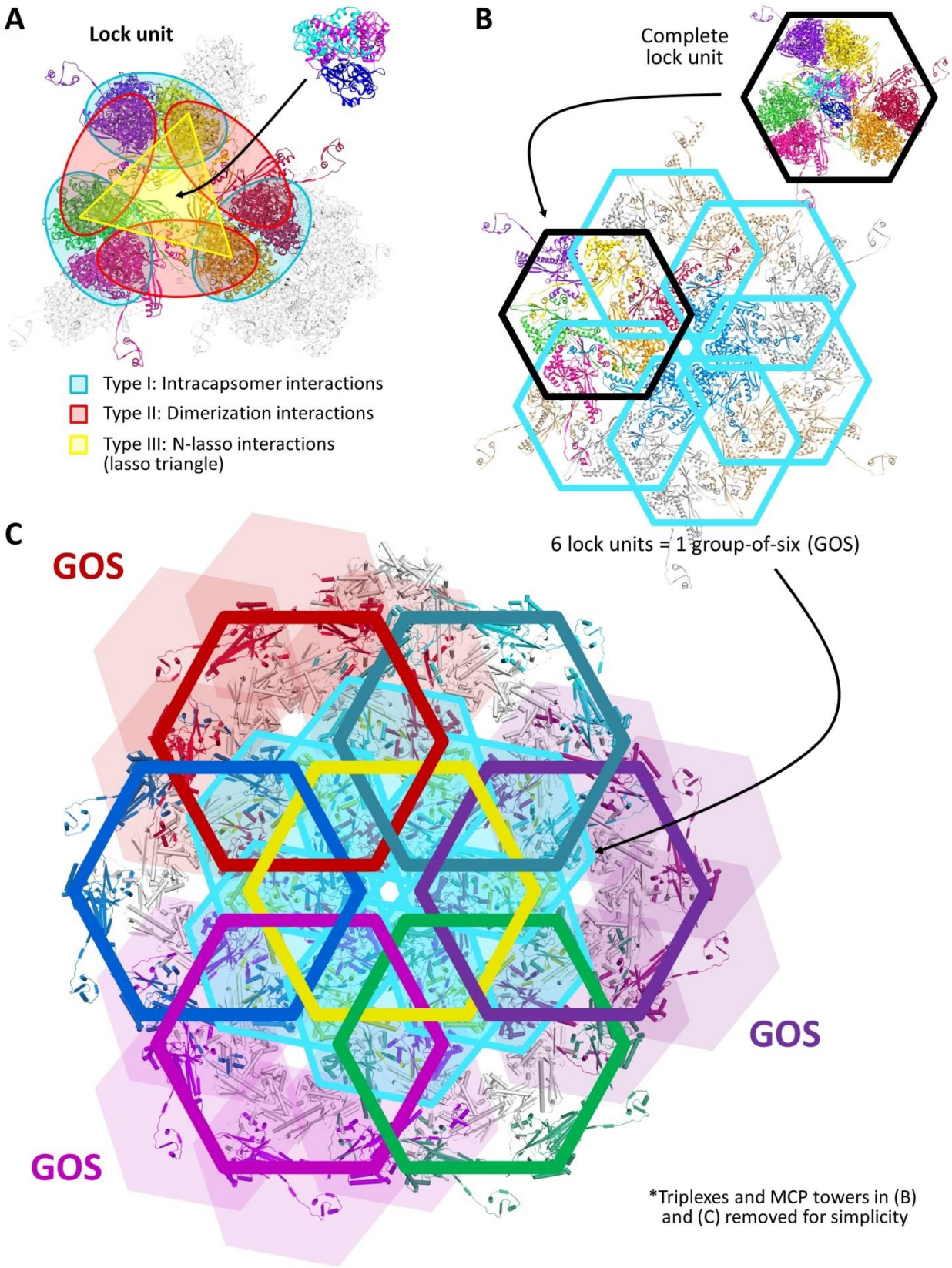
A
Lock unit
Type I: Intracapsomer interactions
Type II: Dimerization interactions
Type III: N-lasso interactions
(lasso triangle)
B
Complete
lock unit
6 lock units = 1 group-of-six (GOS)
C
GOS
GOS
GOS
*Triplexes and MCP towers in (B)
and (C) removed for simplicity

Figure S9. Lock unit interactions and global capsid organization. (A) A lock unit is comprised of six MCPs organized around a central triplex. Each lock unit includes a complete set of all interactions found within the HCMV capsid, including three pairs of type I interactions (blue), three pairs of type II interactions (red), and three pairs of type III interactions forming one lasso triangle (yellow), upon which the triplex sits. **(B)** Lock units are arranged in six overlapping units such that each hexon is at the center of a lock unit group-of-six (GOS). Each MCP is included in two lock units and directly interacts with four lock units. Thus, a lock unit interacts with all lock units within its GOS except the far opposite unit. Intersecting lock unit boundaries denote direct interactions. **(C)** A global view of GOSs reveals that each lock unit (filled hexagons) takes part in three GOSs (blue, teal, and green GOSs not shown for simplicity). Individual lock units are thus able to interact with nine unique lock units—four from each of three GOSs, overlap between GOSs not counted. Concatenated rings representing HK97's covalent chainmail are superposed on overlapping GOSs for comparative reference.

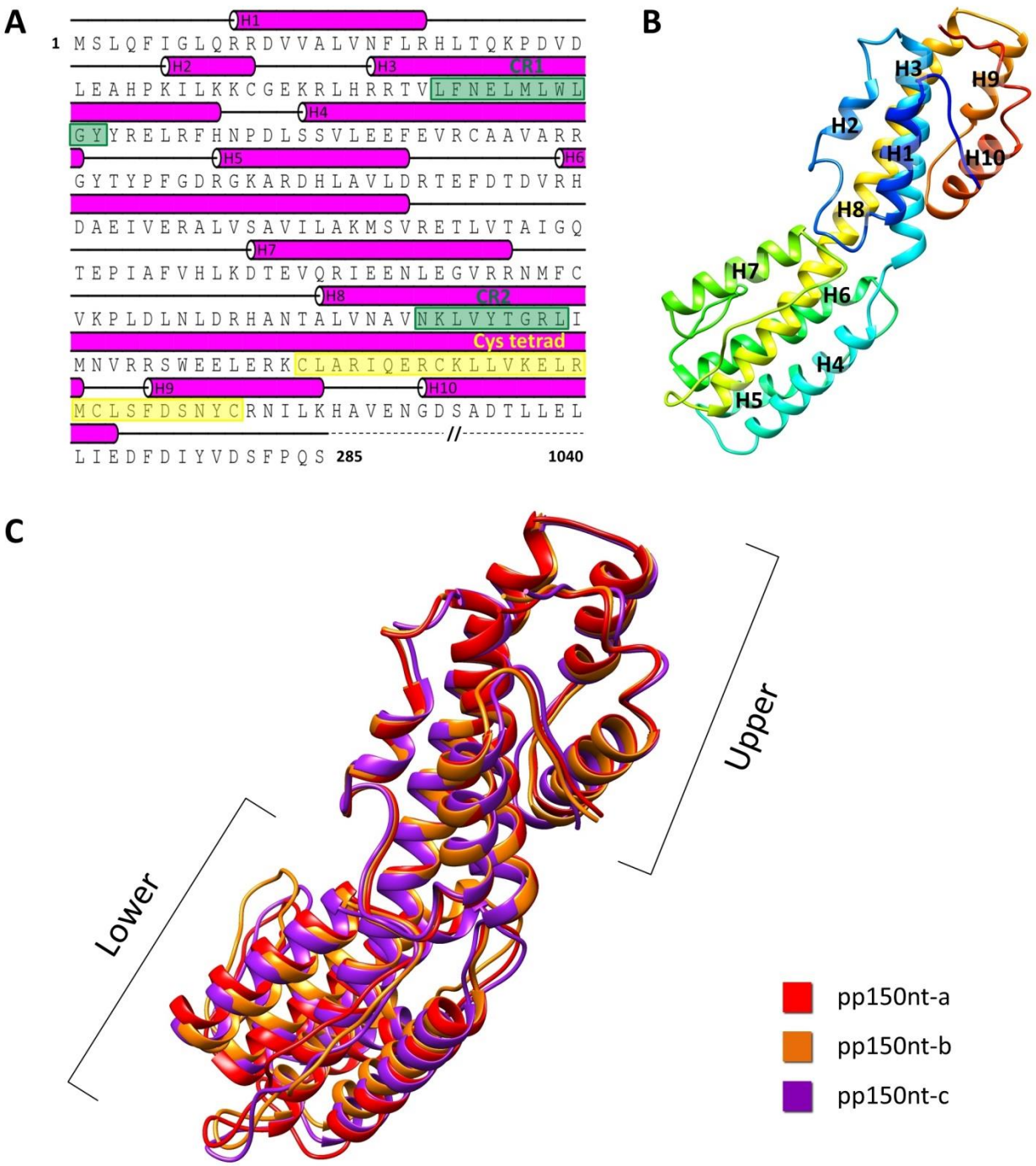

Figure S10. Conserved regions and conformers of pp150nt. (A) Schematic showing the amino acid sequence and secondary structure of pp150nt. Lines represent loops, and pink cylinders represent helices. β-herpesvirus-conserved regions CR1 and CR2 are boxed in green,

while the primate CMV-conserved cysteine tetrad is boxed in yellow. **(B)** Rainbow ribbon model (blue at the N terminus through green and yellow to red at the C terminus) of pp150nt with labeled helices. **(C)** Structural alignment based on Cα positions of the three pp150nt conformers associated with the Tb triplex reveals a greater degree of structural similarity at the upper helix bundle compared to the lower helix bundle.

References and Notes

1. Z. Vancíková, P. Dvorák, Cytomegalovirus infection in immunocompetent and immunocompromised individuals—a review. *Curr. Drug Targets Immune Endocr. Metabol. Disord.* **1**, 179–187 (2001). doi:10.2174/1568005310101020179 Medline

2. S. P. Adler, Congenital cytomegalovirus screening. *Pediatr. Infect. Dis. J.* **24**, 1105–1106 (2005). doi:10.1097/00006454-200512000-00016 Medline

3. C. W. Lerner, M. L. Tapper, Opportunistic infection complicating acquired immune deficiency syndrome. Clinical features of 25 cases. *Medicine* **63**, 155–164 (1984). doi:10.1097/00005792-198405000-00002 Medline

4. D. R. Hoover, A. J. Saah, H. Bacellar, J. Phair, R. Detels, R. Anderson, R. A. Kaslow, Clinical manifestations of AIDS in the era of pneumocystis prophylaxis. Multicenter AIDS Cohort Study. *N. Engl. J. Med.* **329**, 1922–1926 (1993). doi:10.1056/NEJM199312233292604 Medline

5. W. van der Bij, R. Speich, Management of cytomegalovirus infection and disease after solid-organ transplantation. *Clin. Infect. Dis.* **33**, S32–S37 (2001). doi:10.1086/320902 Medline

6. P. Ramanan, R. R. Razonable, Cytomegalovirus infections in solid organ transplantation: A review. *Infect. Chemother.* **45**, 260–271 (2013). doi:10.3947/ic.2013.45.3.260 Medline

7. A. H. Rook, Interactions of cytomegalovirus with the human immune system. *Rev. Infect. Dis.* **10**, S460–S467 (1988). doi:10.1093/clinids/10.Supplement_3.S460 Medline

8. M. J. Cannon, D. S. Schmid, T. B. Hyde, Review of cytomegalovirus seroprevalence and demographic characteristics associated with infection. *Rev. Med. Virol.* **20**, 202–213 (2010). doi:10.1002/rmv.655 Medline

9. E. S. Mocarski, C. T. Courcelle, in *Fields Virology*, vol. 2, D. M. Knipe *et al*., Eds. (Lippincott Williams and Wilkins, 2001), pp. 2629–2674.

10. J. K. Andersen, D. M. Frim, O. Isacson, X. O. Breakefield, Herpesvirus-mediated gene delivery into the rat brain: Specificity and efficiency of the neuron-specific enolase promoter. *Cell. Mol. Neurobiol.* **13**, 503–515 (1993). doi:10.1007/BF00711459 Medline

11. H. Li, X. Zhang, Oncolytic HSV as a vector in cancer immunotherapy. *Methods Mol. Biol.* **651**, 279–290 (2010). doi:10.1007/978-1-60761-786-0_16 Medline

12. S. G. Hansen, J. C. Ford, M. S. Lewis, A. B. Ventura, C. M. Hughes, L. Coyne-Johnson, N. Whizin, K. Oswald, R. Shoemaker, T. Swanson, A. W. Legasse, M. J. Chiuchiolo, C. L. Parks, M. K. Axthelm, J. A. Nelson, M. A. Jarvis, M. Piatak Jr., J. D. Lifson, L. J. Picker, Profound early control of highly pathogenic SIV by an effector memory T-cell vaccine. *Nature* **473**, 523–527 (2011). doi:10.1038/nature10003 Medline

13. S. G. Hansen, M. Piatak Jr., A. B. Ventura, C. M. Hughes, R. M. Gilbride, J. C. Ford, K. Oswald, R. Shoemaker, Y. Li, M. S. Lewis, A. N. Gilliam, G. Xu, N. Whizin, B. J. Burwitz, S. L. Planer, J. M. Turner, A. W. Legasse, M. K. Axthelm, J. A. Nelson, K. Früh, J. B. Sacha, J. D. Estes, B. F. Keele, P. T. Edlefsen, J. D. Lifson, L. J. Picker,

Immune clearance of highly pathogenic SIV infection. *Nature* **502**, 100–104 (2013). doi:10.1038/nature12519 Medline

14. A. J. Davison, A. Dolan, P. Akter, C. Addison, D. J. Dargan, D. J. Alcendor, D. J. McGeoch, G. S. Hayward, The human cytomegalovirus genome revisited: Comparison with the chimpanzee cytomegalovirus genome. *J. Gen. Virol.* **84**, 17–28 (2003). doi:10.1099/vir.0.18606-0 Medline

15. D. Bhella, F. J. Rixon, D. J. Dargan, Cryomicroscopy of human cytomegalovirus virions reveals more densely packed genomic DNA than in herpes simplex virus type 1. *J. Mol. Biol.* **295**, 155–161 (2000). doi:10.1006/jmbi.1999.3344 Medline

16. D. W. Bauer, J. B. Huffman, F. L. Homa, A. Evilevitch, Herpes virus genome, the pressure is on. *J. Am. Chem. Soc.* **135**, 11216–11221 (2013). doi:10.1021/ja404008r Medline

17. M. K. Baxter, W. Gibson, Cytomegalovirus basic phosphoprotein (pUL32) binds to capsids in vitro through its amino one-third. *J. Virol.* **75**, 6865–6873 (2001). doi:10.1128/JVI.75.15.6865-6873.2001 Medline

18. X. Yu, S. Shah, M. Lee, W. Dai, P. Lo, W. Britt, H. Zhu, F. Liu, Z. H. Zhou, Biochemical and structural characterization of the capsid-bound tegument proteins of human cytomegalovirus. *J. Struct. Biol.* **174**, 451–460 (2011). doi:10.1016/j.jsb.2011.03.006 Medline

19. X. Dai, X. Yu, H. Gong, X. Jiang, G. Abenes, H. Liu, S. Shivakoti, W. J. Britt, H. Zhu, F. Liu, Z. H. Zhou, The smallest capsid protein mediates binding of the essential tegument protein pp150 to stabilize DNA-containing capsids in human cytomegalovirus. *PLOS Pathog.* **9**, e1003525 (2013). doi:10.1371/journal.ppat.1003525 Medline

20. P. A. Leong, X. Yu, Z. H. Zhou, G. J. Jensen, Correcting for the ewald sphere in high-resolution single-particle reconstructions. *Methods Enzymol.* **482**, 369–380 (2010). doi:10.1016/S0076-6879(10)82015-4 Medline

21. X. Zhang, Z. H. Zhou, Limiting factors in atomic resolution cryo electron microscopy: No simple tricks. *J. Struct. Biol.* **175**, 253–263 (2011). doi:10.1016/j.jsb.2011.05.004 Medline

22. A. Amunts, A. Brown, X. C. Bai, J. L. Llácer, T. Hussain, P. Emsley, F. Long, G. Murshudov, S. H. Scheres, V. Ramakrishnan, Structure of the yeast mitochondrial large ribosomal subunit. *Science* **343**, 1485–1489 (2014). doi:10.1126/science.1249410 Medline

23. P. Lu, X. C. Bai, D. Ma, T. Xie, C. Yan, L. Sun, G. Yang, Y. Zhao, R. Zhou, S. H. Scheres, Y. Shi, Three-dimensional structure of human γ-secretase. *Nature* **512**, 166–170 (2014). doi:10.1038/nature13567 Medline

24. A. Merk, A. Bartesaghi, S. Banerjee, V. Falconieri, P. Rao, M. I. Davis, R. Pragani, M. B. Boxer, L. A. Earl, J. L. Milne, S. Subramaniam, Breaking cryo-EM resolution barriers to facilitate drug discovery. *Cell* **165**, 1698–1707 (2016). doi:10.1016/j.cell.2016.05.040 Medline

25. D. Veesler, T. S. Ng, A. K. Sendamarai, B. J. Eilers, C. M. Lawrence, S. M. Lok, M. J. Young, J. E. Johnson, C. Y. Fu, Atomic structure of the 75 MDa extremophile *Sulfolobus*

turreted icosahedral virus determined by CryoEM and X-ray crystallography. *Proc. Natl. Acad. Sci. U.S.A.* **110**, 5504–5509 (2013). doi:10.1073/pnas.1300601110 Medline

26. X. Yu, J. Jiang, J. Sun, Z. H. Zhou, A putative ATPase mediates RNA transcription and capping in a dsRNA virus. *eLife* **4**, e07901 (2015). doi:10.7554/eLife.07901 Medline

27. D. Sirohi, Z. Chen, L. Sun, T. Klose, T. C. Pierson, M. G. Rossmann, R. J. Kuhn, The 3.8 Å resolution cryo-EM structure of Zika virus. *Science* **352**, 467–470 (2016). doi:10.1126/science.aaf5316 Medline

28. A. Huet, A. M. Makhov, J. B. Huffman, M. Vos, F. L. Homa, J. F. Conway, Extensive subunit contacts underpin herpesvirus capsid stability and interior-to-exterior allostery. *Nat. Struct. Mol. Biol.* **23**, 531–539 (2016). doi:10.1038/nsmb.3212 Medline

29. X. Dai, D. Gong, Y. Xiao, T. T. Wu, R. Sun, Z. H. Zhou, CryoEM and mutagenesis reveal that the smallest capsid protein cements and stabilizes Kaposi's sarcoma-associated herpesvirus capsid. *Proc. Natl. Acad. Sci. U.S.A.* **112**, E649–E656 (2015). doi:10.1073/pnas.1420317112 Medline

30. Z. H. Zhou, D. H. Chen, J. Jakana, F. J. Rixon, W. Chiu, Visualization of tegument-capsid interactions and DNA in intact herpes simplex virus type 1 virions. *J. Virol.* **73**, 3210–3218 (1999). Medline

31. W. R. Wikoff, L. Liljas, R. L. Duda, H. Tsuruta, R. W. Hendrix, J. E. Johnson, Topologically linked protein rings in the bacteriophage HK97 capsid. *Science* **289**, 2129–2133 (2000). doi:10.1126/science.289.5487.2129 Medline

32. A. Fokine, P. G. Leiman, M. M. Shneider, B. Ahvazi, K. M. Boeshans, A. C. Steven, L. W. Black, V. V. Mesyanzhinov, M. G. Rossmann, Structural and functional similarities between the capsid proteins of bacteriophages T4 and HK97 point to a common ancestry. *Proc. Natl. Acad. Sci. U.S.A.* **102**, 7163–7168 (2005). doi:10.1073/pnas.0502164102 Medline

33. X. Zhang, H. Guo, L. Jin, E. Czornyj, A. Hodes, W. H. Hui, A. W. Nieh, J. F. Miller, Z. H. Zhou, A new topology of the HK97-like fold revealed in *Bordetella* bacteriophage by cryoEM at 3.5 Å resolution. *eLife* **2**, e01299 (2013). doi:10.7554/eLife.01299 Medline

34. M. L. Baker, W. Jiang, F. J. Rixon, W. Chiu, Common ancestry of herpesviruses and tailed DNA bacteriophages. *J. Virol.* **79**, 14967–14970 (2005). doi:10.1128/JVI.79.23.14967-14970.2005 Medline

35. B. R. Bowman, M. L. Baker, F. J. Rixon, W. Chiu, F. A. Quiocho, Structure of the herpesvirus major capsid protein. *EMBO J.* **22**, 757–765 (2003). doi:10.1093/emboj/cdg086 Medline

36. W. W. Newcomb, B. L. Trus, F. P. Booy, A. C. Steven, J. S. Wall, J. C. Brown, Structure of the herpes simplex virus capsid. Molecular composition of the pentons and the triplexes. *J. Mol. Biol.* **232**, 499–511 (1993). doi:10.1006/jmbi.1993.1406 Medline

37. R. Zandi, D. Reguera, Mechanical properties of viral capsids. *Phys. Rev. E Stat. Nonlin. Soft Matter Phys.* **72**, 021917 (2005). doi:10.1103/PhysRevE.72.021917 Medline

38. Z. H. Zhou, J. He, J. Jakana, J. D. Tatman, F. J. Rixon, W. Chiu, Assembly of VP26 in herpes simplex virus-1 inferred from structures of wild-type and recombinant capsids. *Nat. Struct. Biol.* **2**, 1026–1030 (1995). doi:10.1038/nsb1195-1026 Medline

39. L. Lai, W. J. Britt, The interaction between the major capsid protein and the smallest capsid protein of human cytomegalovirus is dependent on two linear sequences in the smallest capsid protein. *J. Virol.* **77**, 2730–2735 (2003). doi:10.1128/JVI.77.4.2730-2735.2003 Medline

40. J. F. Conway, S. K. Cockrell, A. M. Copeland, W. W. Newcomb, J. C. Brown, F. L. Homa, Labeling and localization of the herpes simplex virus capsid protein UL25 and its interaction with the two triplexes closest to the penton. *J. Mol. Biol.* **397**, 575–586 (2010). doi:10.1016/j.jmb.2010.01.043 Medline

41. K. Toropova, J. B. Huffman, F. L. Homa, J. F. Conway, The herpes simplex virus 1 UL17 protein is the second constituent of the capsid vertex-specific component required for DNA packaging and retention. *J. Virol.* **85**, 7513–7522 (2011). doi:10.1128/JVI.00837-11 Medline

42. X. Dai, D. Gong, T. T. Wu, R. Sun, Z. H. Zhou, Organization of capsid-associated tegument components in Kaposi's sarcoma-associated herpesvirus. *J. Virol.* **88**, 12694–12702 (2014). doi:10.1128/JVI.01509-14 Medline

43. U. Sae-Ueng, T. Liu, C. E. Catalano, J. B. Huffman, F. L. Homa, A. Evilevitch, Major capsid reinforcement by a minor protein in herpesviruses and phage. *Nucleic Acids Res.* **42**, 9096–9107 (2014). doi:10.1093/nar/gku634 Medline

44. D. P. AuCoin, G. B. Smith, C. D. Meiering, E. S. Mocarski, Betaherpesvirus-conserved cytomegalovirus tegument protein ppUL32 (pp150) controls cytoplasmic events during virion maturation. *J. Virol.* **80**, 8199–8210 (2006). doi:10.1128/JVI.00457-06 Medline

45. J. Kindt, S. Tzlil, A. Ben-Shaul, W. M. Gelbart, DNA packaging and ejection forces in bacteriophage. *Proc. Natl. Acad. Sci. U.S.A.* **98**, 13671–13674 (2001). doi:10.1073/pnas.241486298 Medline

46. A. Evilevitch, L. Lavelle, C. M. Knobler, E. Raspaud, W. M. Gelbart, Osmotic pressure inhibition of DNA ejection from phage. *Proc. Natl. Acad. Sci. U.S.A.* **100**, 9292–9295 (2003). doi:10.1073/pnas.1233721100 Medline

47. Z. H. Zhou, J. Chiou, Protein chainmail variants in dsDNA viruses. *AIMS Biophys.* **2**, 200–218 (2015). doi:10.3934/biophy.2015.2.200

48. A. A. Rizzo, M. M. Suhanovsky, M. L. Baker, L. C. Fraser, L. M. Jones, D. L. Rempel, M. L. Gross, W. Chiu, A. T. Alexandrescu, C. M. Teschke, Multiple functional roles of the accessory I-domain of bacteriophage P22 coat protein revealed by NMR structure and CryoEM modeling. *Structure* **22**, 830–841 (2014). doi:10.1016/j.str.2014.04.003 Medline

49. G. C. Lander, A. Evilevitch, M. Jeembaeva, C. S. Potter, B. Carragher, J. E. Johnson, Bacteriophage lambda stabilization by auxiliary protein gpD: Timing, location, and mechanism of attachment determined by cryo-EM. *Structure* **16**, 1399–1406 (2008). doi:10.1016/j.str.2008.05.016 Medline

50. B. Carragher, N. Kisseberth, D. Kriegman, R. A. Milligan, C. S. Potter, J. Pulokas, A. Reilein, Leginon: An automated system for acquisition of images from vitreous ice specimens. *J. Struct. Biol.* **132**, 33–45 (2000). doi:10.1006/jsbi.2000.4314 Medline

51. C. Suloway, J. Pulokas, D. Fellmann, A. Cheng, F. Guerra, J. Quispe, S. Stagg, C. S. Potter, B. Carragher, Automated molecular microscopy: The new Leginon system. *J. Struct. Biol.* **151**, 41–60 (2005). doi:10.1016/j.jsb.2005.03.010 Medline

52. X. Li, P. Mooney, S. Zheng, C. R. Booth, M. B. Braunfeld, S. Gubbens, D. A. Agard, Y. Cheng, Electron counting and beam-induced motion correction enable near-atomic-resolution single-particle cryo-EM. *Nat. Methods* **10**, 584–590 (2013). doi:10.1038/nmeth.2472 Medline

53. J. A. Mindell, N. Grigorieff, Accurate determination of local defocus and specimen tilt in electron microscopy. *J. Struct. Biol.* **142**, 334–347 (2003). doi:10.1016/S1047-8477(03)00069-8 Medline

54. Y. Liang, E. Y. Ke, Z. H. Zhou, IMIRS: A high-resolution 3D reconstruction package integrated with a relational image database. *J. Struct. Biol.* **137**, 292–304 (2002). doi:10.1016/S1047-8477(02)00014-X Medline

55. S. J. Ludtke, P. R. Baldwin, W. Chiu, EMAN: Semiautomated software for high-resolution single-particle reconstructions. *J. Struct. Biol.* **128**, 82–97 (1999). doi:10.1006/jsbi.1999.4174 Medline

56. X. Zhang, X. Zhang, Z. H. Zhou, Low cost, high performance GPU computing solution for atomic resolution cryoEM single-particle reconstruction. *J. Struct. Biol.* **172**, 400–406 (2010). doi:10.1016/j.jsb.2010.05.006 Medline

57. P. B. Rosenthal, R. Henderson, Optimal determination of particle orientation, absolute hand, and contrast loss in single-particle electron cryomicroscopy. *J. Mol. Biol.* **333**, 721–745 (2003). doi:10.1016/j.jmb.2003.07.013 Medline

58. A. Kucukelbir, F. J. Sigworth, H. D. Tagare, Quantifying the local resolution of cryo-EM density maps. *Nat. Methods* **11**, 63–65 (2014). doi:10.1038/nmeth.2727 Medline

59. Y. Wan, W. Chiu, Z. H. Zhou, in *2004 International Conference on Communications, Circuits and Systems* (Institute of Electrical and Electronics Engineers, 2004), pp. 960–964.

60. Z. H. Zhou, Atomic resolution cryo electron microscopy of macromolecular complexes. *Adv. Protein Chem. Struct. Biol.* **82**, 1–35 (2011). doi:10.1016/B978-0-12-386507-6.00001-4 Medline

61. D. J. DeRosier, Correction of high-resolution data for curvature of the Ewald sphere. *Ultramicroscopy* **81**, 83–98 (2000). doi:10.1016/S0304-3991(99)00120-5 Medline

62. E. F. Pettersen, T. D. Goddard, C. C. Huang, G. S. Couch, D. M. Greenblatt, E. C. Meng, T. E. Ferrin, UCSF Chimera—a visualization system for exploratory research and analysis. *J. Comput. Chem.* **25**, 1605–1612 (2004). doi:10.1002/jcc.20084 Medline

63. P. Emsley, K. Cowtan, Coot: Model-building tools for molecular graphics. *Acta Crystallogr. D Biol. Crystallogr.* **60**, 2126–2132 (2004). doi:10.1107/S0907444904019158 Medline

64. A. Drozdetskiy, C. Cole, J. Procter, G. J. Barton, JPred4: A protein secondary structure prediction server. *Nucleic Acids Res.* **43**, W389–W394 (2015). doi:10.1093/nar/gkv332 Medline

65. L. A. Kelley, S. Mezulis, C. M. Yates, M. N. Wass, M. J. Sternberg, The Phyre2 web portal for protein modeling, prediction and analysis. *Nat. Protoc.* **10**, 845–858 (2015). doi:10.1038/nprot.2015.053 Medline

66. P. D. Adams, P. V. Afonine, G. Bunkóczi, V. B. Chen, I. W. Davis, N. Echols, J. J. Headd, L. W. Hung, G. J. Kapral, R. W. Grosse-Kunstleve, A. J. McCoy, N. W. Moriarty, R. Oeffner, R. J. Read, D. C. Richardson, J. S. Richardson, T. C. Terwilliger, P. H. Zwart, *PHENIX*: A comprehensive Python-based system for macromolecular structure solution. *Acta Crystallogr. D Biol. Crystallogr.* **66**, 213–221 (2010). doi:10.1107/S0907444909052925 Medline